

PAPER • OPEN ACCESS

Noise Propagation Calculations of a Wind Turbine in Complex Terrain

To cite this article: Matias Sessarego and Wen Zhong Shen 2020 *J. Phys.: Conf. Ser.* **1452** 012063

View the [article online](#) for updates and enhancements.



IOP | ebooks™

Bringing you innovative digital publishing with leading voices to create your essential collection of books in STEM research.

Start exploring the [collection](#) - download the first chapter of every title for free.

Noise Propagation Calculations of a Wind Turbine in Complex Terrain

Matias Sessarego and Wen Zhong Shen

Fluid Mechanics Section, Department of Wind Energy, Technical University of Denmark, 2800 Kongens Lyngby, Denmark

E-mail: matse@dtu.dk

Abstract. This paper describes numerical noise propagation calculations of a single wind turbine in complex terrain near a town in Central Denmark. The purpose of the work is to estimate the noise level at increasing distances from a single wind turbine and investigate the effect of complex terrain. Results indicate that time varying numerical noise propagation predictions of wind turbines in complex terrain can be achieved by using computational fluid dynamics via large-eddy simulation (LES) and the Technical University of Denmark's noise propagation tool based on the parabolic equation. The wind turbine is modeled using the actuator line approach. The results from this project will have significant social, environmental, and economic impact, since accurate predictions of wind turbine noise propagation can be used to develop noise mitigation strategies to increase the public acceptance of wind energy.

1. Introduction

One of the main obstacles in the public acceptance of wind energy is wind turbine noise [1]. Studies have been carried out on the topic, for example, the human response to wind turbine noise and the reasons for the higher annoyance of wind turbine noise compared to other noise sources [2, 3]. Regulations have been put forth, such as the Danish wind turbine noise regulation [4], that limits the noise impact from wind turbines. However, such regulations may be too conservative and have an adverse effect on the energy yield of wind farms. These regulations may limit the number of new wind farms being developed on land as well. More wind turbine noise measurement campaigns must be conducted and further development of numerical tools for predicting wind turbine noise are needed to revise the regulations.

Previous work on numerical investigations of wind turbine noise involving propagation are found in [5–10]. Zhu et al. [5] employed computational fluid dynamics (CFD) and the actuator disc approach together with wind turbine noise source generation and sound propagation models. The CFD employed was specifically a Reynolds-Averaged Navier-Stokes (RANS) solver. The noise source generation method was based on the semi-empirical airfoil self-noise model of Brooks et al. [11] while the propagation was solved using the Parabolic Equation (PE) in the frequency domain. Similarly, Shen et al. [6] employed the same models as in [5] but for a complex terrain site in China. Cao et al. [7] modeled wind farm noise by using a wake model, semi-empirical wind turbine noise source model, and solving the parabolic wave equation. Heimann, Englberger and Schady [8] investigated the sound propagation of a wind turbine on a hill based on numerical



simulations by coupling a Large-Eddy Simulation (LES) flow model as precursor to a three-dimensional (3D) ray-based sound particle model. Heimann and Englberger [9] later used the models to study the impact of the diurnal variability on sound propagation through the wind turbine wake. Sessarego [10] developed a noise propagation database based on LES, the actuator line (AL) approach, and PE propagation in flat terrain.

This paper describes numerical noise propagation calculations of a single wind turbine in a three-dimensional complex terrain environment near a town in Central Denmark. The present work differs from [5,6] in that the LES approach is used instead of RANS and differs from [5] also because a complex terrain site is considered instead of flat ground. Cao et al. [7] does not consider complex terrain or use high-fidelity CFD approaches such as RANS or LES for modeling the flow field. In comparison with [8,9], a more advanced PE model is used as the propagation model instead of a ray-based model. Also, an actual complex terrain site is considered. However, the PE model in this work uses a two-dimensional (2D) axisymmetric approach for treating 3D problems as a full 3D PE requires a substantial computing resource. Previous work from the author [10] was only based on flat terrain.

The purpose of the work is to estimate the noise level at increasing distances downstream from a single wind turbine including the effect of complex terrain using high-fidelity tools: LES and PE. The work described in this paper represents a small portion of a large project on research and development of wind turbine noise. The project is expected to have significant social, environmental, and economic impact. For example, accurate predictions of wind turbine noise source and propagation can be used to develop noise mitigation strategies in terms of control and in the development of new wind farms. The developments from this project are aimed at decreasing the impact of wind turbine noise and increasing the public acceptance of wind energy.

A brief description of the methods used will be described first in section 2. Then, results from the noise propagation will be shown in section 3. Finally, conclusions are given in section 4.

2. Methodology

The methodology consists of a description of the terrain map in subsection 2.1, wind turbine flow solver in subsection 2.2, and wind turbine noise solver in subsection 2.3.

2.1. Terrain map

The DHM (Danmarks Højdemodel)-2007 1.6 m grid terrain data from [12] was used. The DHM-Terrain is a model of elevation on the surface of terrain. Buildings, vegetation and cars have been removed from the model. The model is stored in a grid with a cell size of 1.6 meters. The model is suitable for planning, design and landscape analyses. An ASC format data file with a 10 by 10 km block is extracted in the UTM32-ETRS89 coordinate system, see Figure 1. UTM/ETRS89 (formerly EUREF89) is the primary map projection in Denmark for the exchange, storage and processing of geodata. Zone 32 covers all of Denmark except Bornholm. The data is delivered in ASCII GRID, which is an uncompressed raster format belonging to ArcGIS (ESRI) and is read through a number of GIS systems.

A smaller square domain with a size of $X/R = 15$ or $Y/R = 15$ is selected for the CFD and noise propagation computations. The domain is made non-dimensional by dividing the distance by the rotor radius. Figure 2 depicts the non-dimensional terrain map, wind turbine location and lines of interest for noise propagation calculations in two views: (a) from top and (b) in three dimensions. The lines of interest were selected to study the effect of the wind turbine wake downstream of the turbine. The dashed line represents upstream/downstream of the turbine and the diagonal line is at a 50 degree angle away from the wind/wake direction. The wind travels from the left and towards the right in the positive Z direction in Figure 2(a).

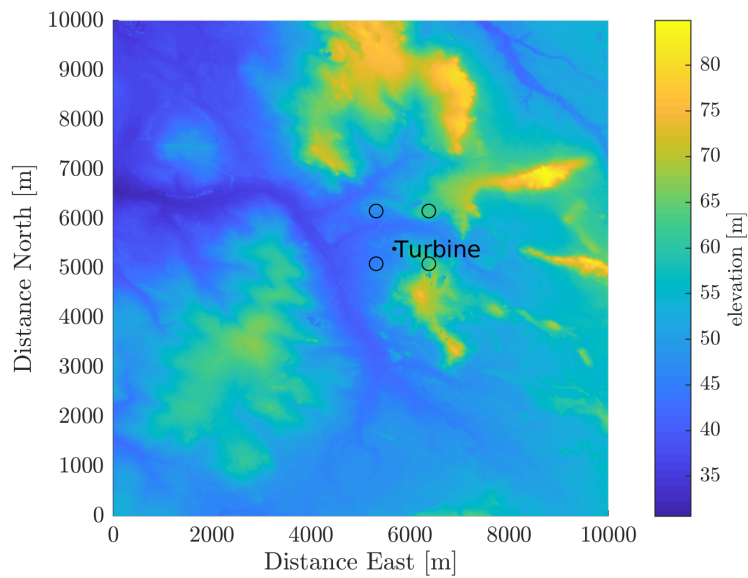


Figure 1: Terrain map of a 10 by 10 km block containing the wind turbine location and square area of interest bounded by the four vertices depicted as hollow circles.

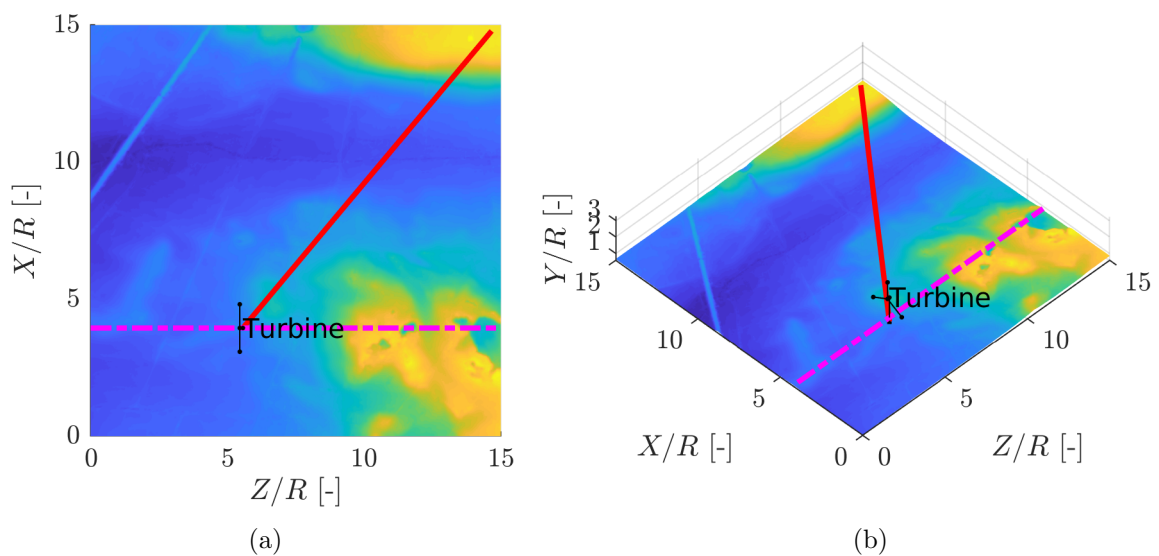


Figure 2: Non-dimensional terrain map, wind turbine location and lines of interest for noise propagation calculations in two views: (a) from top and (b) in three dimensions.

2.2. Wind turbine flow solver

Before noise computations are carried out, flow simulations are performed to provide the flow input to the noise propagation models. This section describes the simulation tool and models used to generate the flow inputs in two subsections. Subsection 2.2.1 describes the general purpose flow solver and subsection 2.2.2 describes the wind turbine model used to represent the wind turbine within the flow domain. Subsection 2.2.3 describes the computational setup to execute the flow solver to obtain the flow fields.

2.2.1. Flow field The flow is governed by the Navier-Stokes equations and simulations are performed using a CFD solver typically based on either the RANS or LES approaches. Flow fields from LES computations are used since it allows the noise propagation model to capture the effects of noise from some of the different turbulent scales in the time domain. The different turbulence scales in the flow are relevant because they are responsible for the noise generation in turbulent flow induced noise and have an impact on noise propagation.

The in-house EllipSys3D [13, 14] code developed at the Technical University of Denmark (DTU) is employed in the current work for generating the flow fields. EllipSys3D is a general purpose flow solver based on a structured grid topology, with a multi-block and cell-centered finite volume discretization. The Navier-Stokes equations are solved either steady or unsteady using the pressure-velocity coupling technique where the predictor-corrector method is used. The EllipSys3D code is programmed with a multi-block topology and is parallelized using Message Passage Interface (MPI). Both the RANS and LES techniques are implemented in EllipSys3D, however only the filtered Navier-Stokes LES equations are being solved numerically in the current study. Last, only neutral atmospheric stability conditions are considered in the flow simulations.

2.2.2. Wind turbine model To include the effects of the wind turbine wake and unsteady moving sources on noise propagation, a wind turbine rotor model is required in the wind turbine flow solver. The AL technique as described in [15] is employed in the current work, where the wind turbine rotor blades are represented by rotating lines. By using the AL technique within EllipSys3D, complex flow conditions on the wind turbine can be modeled, such as turbulent inflow, wind shear and yaw, etc. To compute the flow field over the wind turbine blades, a volume body force is added to the momentum equation. The body force is computed iteratively with the blade element approach with tabulated airfoil lift and drag data, e.g. lift (CL) and drag (CD) coefficients. The AL approach is coupled with the in-house developed aero-elastic code FLEX5 [16, 17]. The coupling with FLEX5 allows the addition of the wind turbine pitch and rotor RPM controllers as well as the flexibility of the turbine components, e.g. blades, tower, shaft, etc., within the simulation. The wind turbine flexibility and controller dynamics have been included in the simulations.

The wind turbine model is a virtual one with a power rating of 4.1 MW. This virtual wind turbine was chosen as an approximation to the actual turbine with the same rating at the site. Blade chord, twist, thickness and airfoil lift and drag coefficients are based on the National Renewable Energy Laboratory's (NREL) 5 MW wind turbine [18]. Measurements of pitch and rotor RPM of the actual wind turbine are used to determine the pitch and rotor RPM schedules. For confidentiality reasons, further details on the virtual wind turbine model cannot be provided even though it is mostly based on the NREL 5 MW design.

2.2.3. Flow solver setup Figure 3 depicts the mesh comprised of 1188 blocks where each block contains 48^3 cells. The mesh is rectangular in shape and the square domain at the center containing the terrain profile is 18×18 blocks in width and length. The terrain profile is discussed in detail in subsection 2.1.

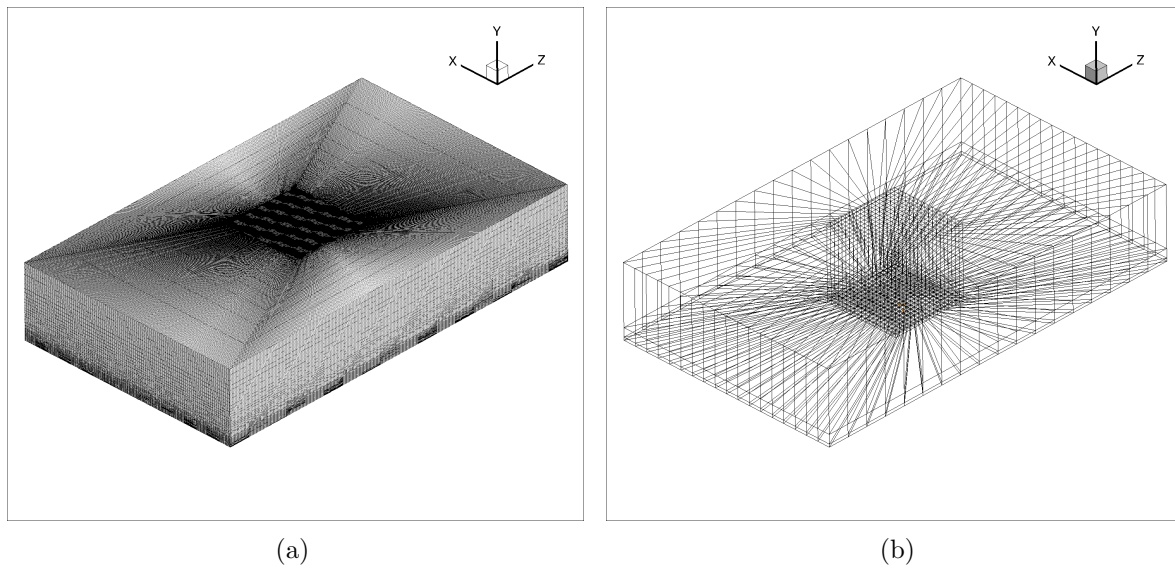


Figure 3: (a) Computational grid and (b) block structure used in the AL-LES computations.

The computational mesh is designed such that there is more grid points at the center to capture terrain effects and the effect of the actuator lines on the flow field. Further away from the center and towards the boundary of the mesh, a much coarser grid is used over a long distance to minimize the computational cost and at the same time reduce the effect of the boundary conditions on the flow field at the center. The disturbances in the flow at the center will persist up to a certain distance away all around. Therefore, it is important to place the computational boundaries far enough so that the flow will have attained free stream conditions again. If the far-field distances are placed at closer distances, the boundary conditions applied on the far field will suppress the flow field variations at the center, which will lead to erroneous results from the computations. The computational grid has approximately 60 (horizontal) and 56 (vertical) grid points on the rotor swept area. The resulting grid density is higher than the one used in previous work [19]. The AL-LES computation is performed using two-hundred-and-ninety-seven 2.8 GHz processors on a Linux cluster, where each processor is allocated for four blocks out of the 1188 blocks, i.e., $297 \times 4 = 1188$ blocks.

Figure 4 depicts two views of the boundary conditions applied on the mesh from the (a) front-top and (b) rear-bottom where the no-slip, inlet, far-field, and outlet boundary conditions or attributes (attr) are color-coded as 101 (dark blue), 201 (light blue), 301 (green), and 401 (yellow), respectively. The flow field in the entire domain during the CFD computation is normalized by a user-specified wind speed value, which is 6.5 m/s for the simulations shown in this work. The user-specified wind speed value is referenced to a data point measured at one rotor radius, R , in front of the wind turbine hub height. In other words, the inflow wind speed is approximately 6.5 m/s. A power-law wind shear profile [20] is prescribed at the first time step using an arbitrary shear exponent of 0.1. In practice, the shear exponent should be estimated from the ground and weather conditions at the site, which has been omitted in the current study. Unsteady simulations are performed for a 2-minute time period in real time (136 seconds to be exact). The computational time from start to finish is approximately 64 hours. Flow fields from the AL-LES computations are shown in section 3.

Synthetic inflow turbulence is simulated by prescribing a plane, 1065×568 m in width and height, respectively, where the bottom-right corner of the plane is placed at $X = Y = Z = 0$, see Figure 2. In other words, the plane is situated at $Z = 0$ and covers the entire width of the

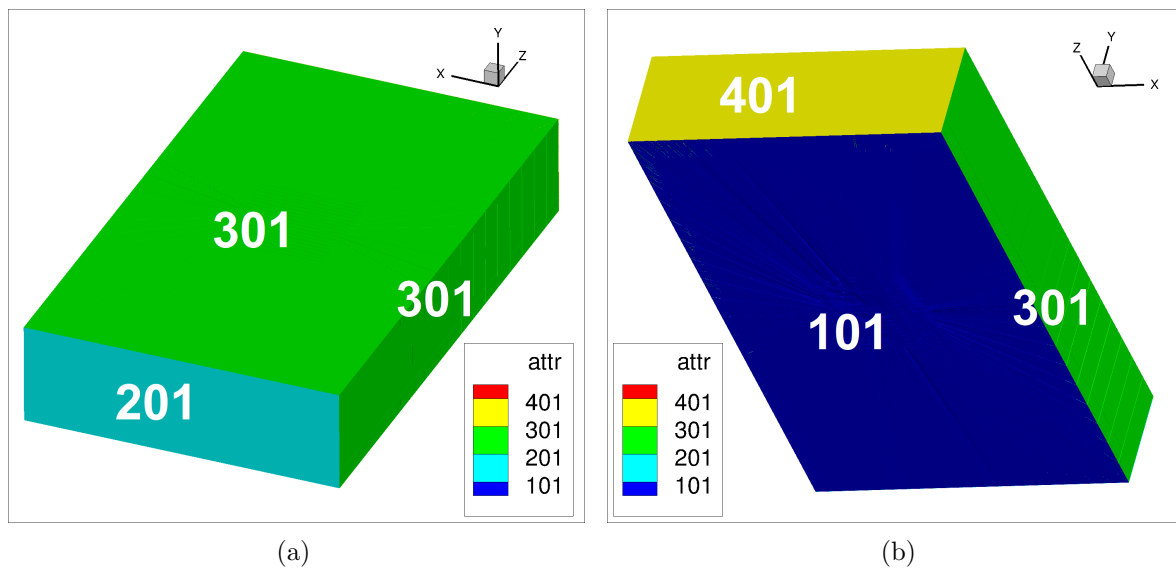


Figure 4: Two views of the boundary conditions applied on the mesh from the (a) front-top and (b) rear-bottom where the no-slip, inlet, far-field, and outlet boundary conditions or attributes (attr) are color-coded as 101 (dark blue), 201 (light blue), 301 (green), and 401 (yellow), respectively.

terrain from $X = 0$ to $X = 15$ and from $Y = 0$ to $Y = 8$ for the height. Turbulence boxes are generated as a pre-processing step using the Mann model [21, 22] and slices from the box are gradually fed into the plane during the simulation.

2.3. Wind turbine noise solver

The wind turbine noise solver is comprised of the noise propagation model only. Including a noise source model based on Brooks et al. [23] is possible but is not used in the current study for brevity. This section describes the noise propagation model and setup in subsections 2.3.1 and 2.3.2, respectively.

2.3.1. Noise propagation model Predictions of wind turbine noise propagation can be made with various analytical and numerical modeling techniques, see [24] for a review. For example, there is a variety of ray tracing formulations available, which are analytical approaches based on geometrical acoustic theory. However, when considering complicated terrain topography and flow conditions such as the ones involved in the current study, numerical approaches based on parabolic equations are more suitable to the problem.

A 2D PE model is employed in the current work. The PE method is a solution to the acoustic wave equation with approximations of harmonic wave propagations with a finite angle and a preferred direction of propagation. In this study, the 2D, wide-angle, Crank-Nicholson PE is used with the starter function and implementation details given in [25]. In this method the moving atmosphere is replaced by a hypothetical motionless medium with an effective speed of sound, $c_{eff} = c + v_x$, where v_x is the wind velocity component along the direction between source and receiver [26]. The wind velocity components are obtained from the flow solver described in section 2.2. The solution of each PE simulation yields a steady solution at each frequency. Since a time dependent solution is desired in the present work, multiple PE simulations are performed successively to capture the relative sound pressure level (SPL) as a function of time.

The 2D PE model is obtained with a number of assumptions and some of the limitations will

be described here. First, a 2D approach for sound propagation modeling in a vertical plane is employed, which neglects azimuth refraction. In an undisturbed atmosphere in flat terrain with no obstacles the 2D approach is valid, since the wind and temperature gradients in the vertical plane dominate and thus azimuth refraction is negligible [9]. However, azimuth gradients exist in the case of the present work because an obstacle, i.e., a wind turbine, and a complex terrain environment with hills is considered. In the paper of Cheng et al. [27], the effects between 2D PE and 3D PE were analysed for upwind, cross-wind and down propagation with a source height of 3.4 m and 68 m. Some differences were reported on the locations of propagation peaks and troughs at large distances. However, these differences should be very much reduced when the atmospheric turbulence is included in PE. Second, the PE model is a one-way propagation method, which means that back-scattering is neglected. Third, the wide-angle implementation of the parabolic wave equation is only valid within ± 35 degrees in the paraxial direction [28]. The second limitation is usually not the case for wind turbines and the third one becomes an issue only if the area of interest is close to both the ground and an elevated source, e.g., a wind turbine.

The PE model has been studied extensively by Barlas et al. [29–31] for single wind turbine noise propagation on flat terrain using a variety of inputs and simulation scenarios. In these studies, the effects of wind shear, different turbulence intensity levels and source modeling approaches are investigated. At DTU, the PE model is incorporated into a general purpose noise propagation tool called WindSTAR-Pro (Wind turbine Simulation Tool for Aerodynamic noise Propagation) [32].

2.3.2. Noise propagation setup The sound emission from each wind turbine blade can be approximated by a lumped point source on the outer part of each blade, but not at the tip, e.g., at 80% of the blade span. This approximation is based on the source location studies in [1], which states that the sound is produced in the outer part of the blades. Therefore, the source locations are calculated based on 80% of the span of each AL. Figure 7 depicts the source locations shown on top of the wind speed contour upstream/downstream of the wind turbine.

Then, the relative sound pressure level is computed by performing 2D-PE simulations at 2D planes within the domain between the source on each blade and two receivers. The two receivers are located at the endpoints of the lines of interest, see Figure 2. For the Crank-Nicholson PE calculations, the spatial resolution for both horizontal and vertical directions on the 2D-plane is set to one-eighth of the wavelength, i.e., $\delta x = \delta y = \lambda/8$, where λ is the wavelength of the solving frequency. The terrain profile along the 2D plane is interpolated from the terrain grid and the ground impedance was defined using the theoretical and four-parameter model of Attenborough [33]. An effective flow resistivity value of 250 kPa s/m² was chosen based on an estimate of the conditions for the site described in subsection 2.1.

All simulations are carried out for 1/3 octave band center frequencies, f_i , from 50 Hz to 1000 Hz. Frequencies higher than 1000 Hz are assumed to have a negligible contribution to the overall SPL due to atmospheric absorption. The sound pressure level, L_p , is defined by Equation 1:

$$L_p(f_i) = L_W(f_i) - 10 \log_{10} 4\pi r^2 - \alpha r + \Delta L \quad (1)$$

where L_W is the sound power level, r is the radial distance from the source, α is the atmospheric absorption coefficient, and ΔL is the relative sound pressure level. In the current study, only ΔL is considered in the analyses for simplicity and brevity. In other words, the sound power level, geometrical attenuation, and atmospheric absorption terms in Equation 1 are neglected. As mentioned in subsection 2.3, the sound power level can be obtained from the noise source model based on Brooks et al. [23]. Including the geometrical attenuation and atmospheric absorption is straightforward. The relative sound pressure level in each band are summed logarithmically

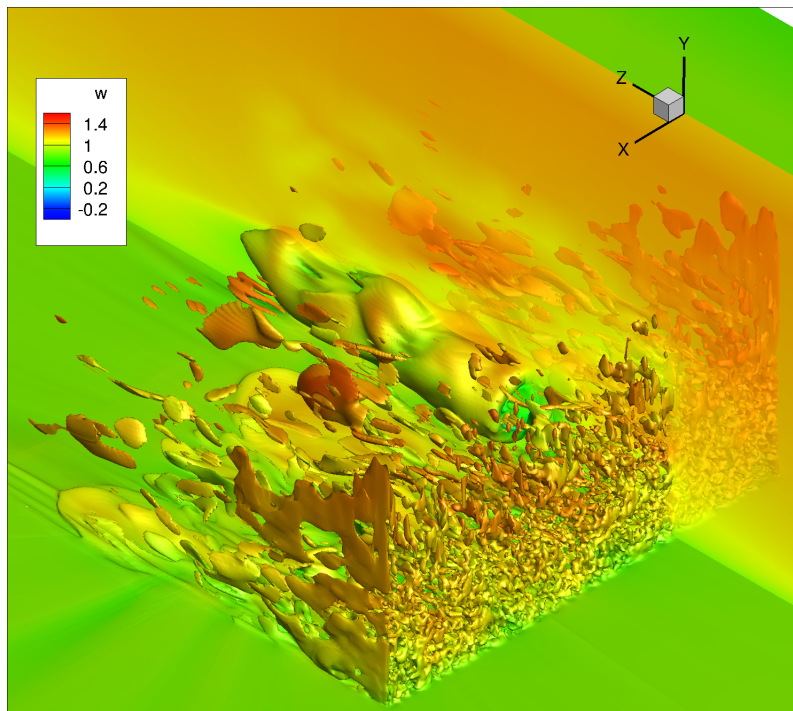


Figure 5: Iso-surface of vorticity and two-dimensional slice with normalized streamwise windspeed, w , for the actuator line large-eddy simulation of a wind turbine in complex terrain with synthetic inflow turbulence and 6.5 m/s wind speed.

to obtain the overall relative sound pressure level, ΔL_{sum} , as defined in Equation 2:

$$\Delta L_{\text{sum}} = 10 \log_{10} \left(\sum_{i=1}^N 10^{\Delta L_i/10} \right) \quad (2)$$

where N is the number of frequencies used.

3. Results

Figure 5 depicts the iso-surface of vorticity of the actuator line large-eddy simulation (AL-LES). A 2D slice showing the normalized streamwise windspeed, w , is also shown in the figure. Figure 6 depicts the extraction for the wind velocity from the wind turbine flow solver used as input to the noise propagation model. In Figure 6, approximately 32 million data points are extracted from the grid, i.e., $401 \times 201 \times 401$ points in the X , Y , and Z directions, respectively. Figure 7 depicts a contour of the wind speed upstream and downstream of the wind turbine derived from 401×201 data points on a 2D slice in the AL-LES computation. The source locations shown in Figure 7 were projected on the 2D plane for visibility since they lie outside of the plane. Slices from the flow field are used to generate the 2D wind velocity planes between the source and receiver along the lines of interest, see subsection 2.1. The 2D wind velocity planes are used as input for noise propagation calculations.

Figures 8 and 9 depict the wind velocity and overall relative SPL on the 2D planes, respectively, including the terrain topography. The actuator lines and source locations are shown in the figures as well. The 2D planes are between each of the sources on the blades and the two receivers located at the endpoints for both the diagonal and upstream/downstream lines of interest, see subsection 2.1. These endpoints are approximately 600 m to 1.1 km away from the turbine as seen in Figure 2.

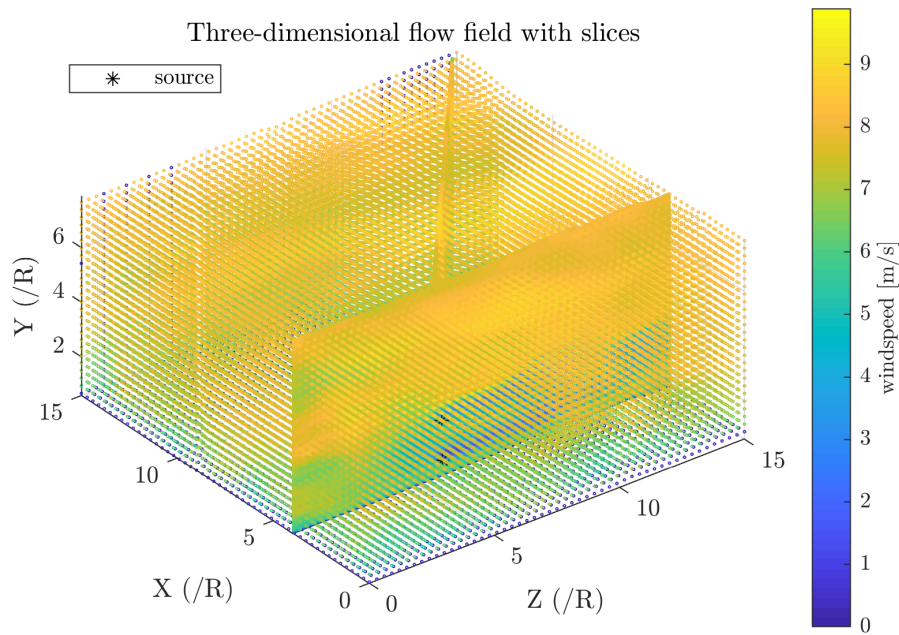


Figure 6: Wind velocity extraction from flow solver for input to the noise propagation model.

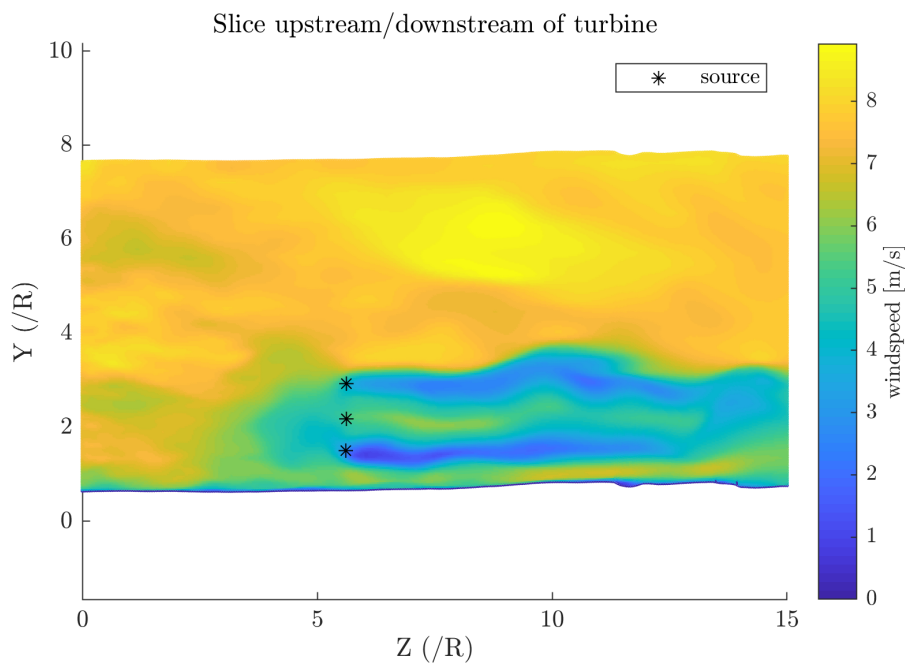


Figure 7: Contour of the wind speed upstream and downstream of the wind turbine in the AL-LES computation and source locations.

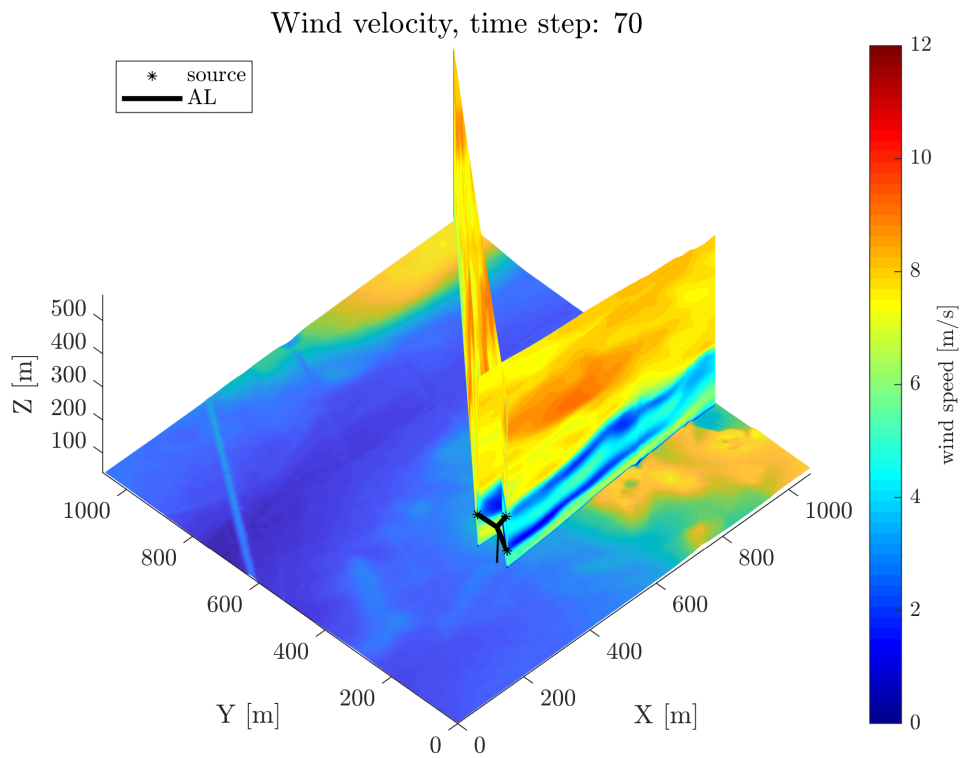


Figure 8: Wind velocity on 2D planes between source and receiver including the terrain map.

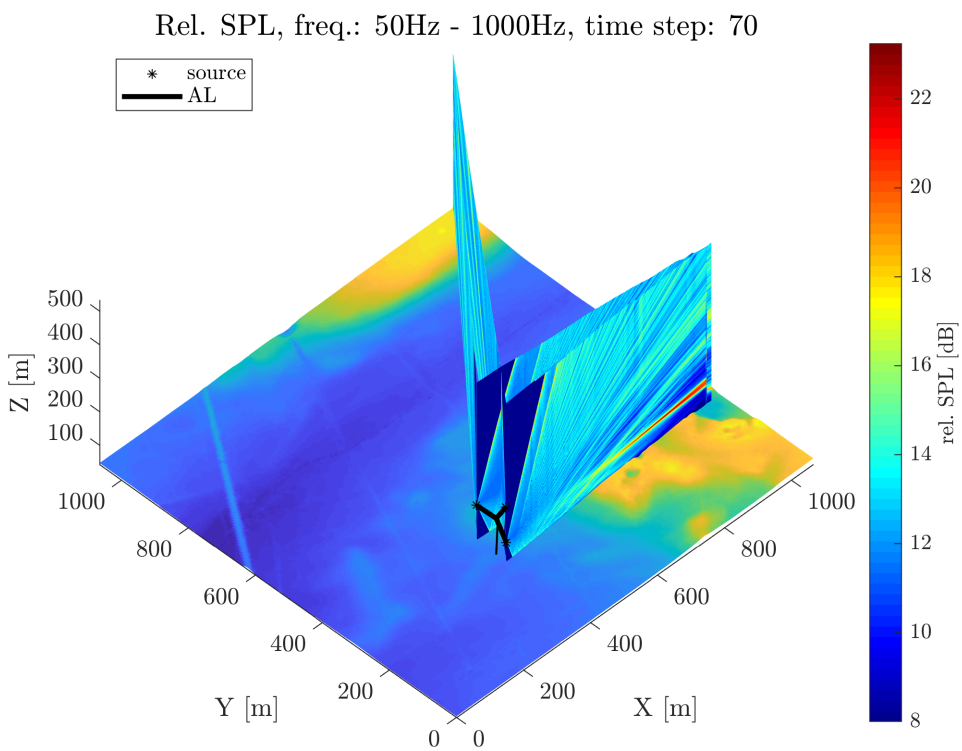


Figure 9: Overall relative sound pressure level (rel. SPL) computed from the PE model on 2D planes between source and receiver including the terrain map.

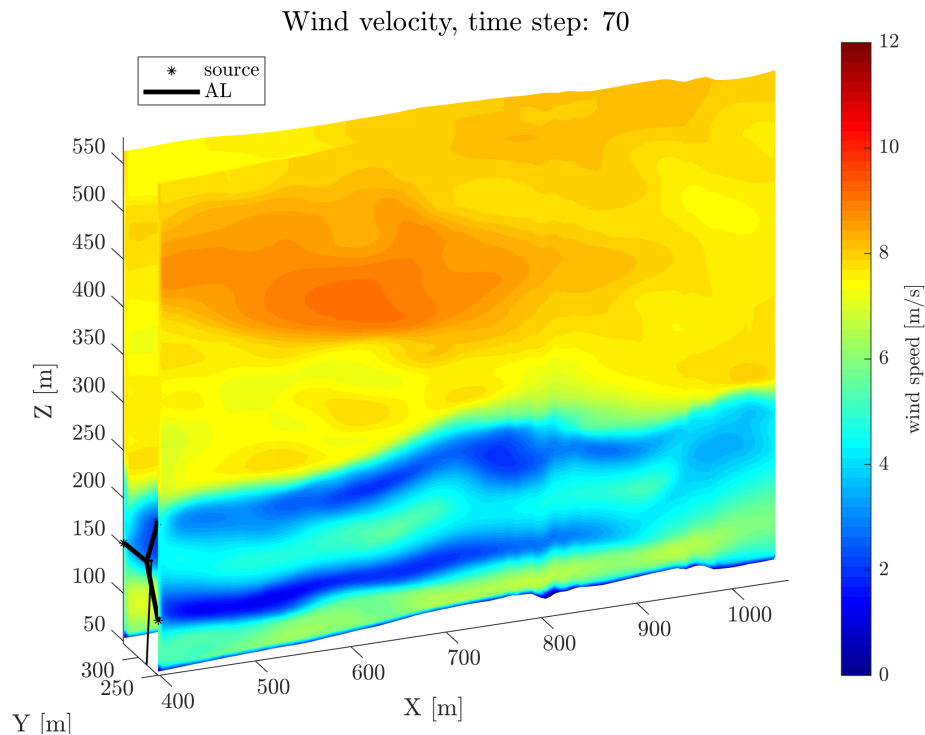


Figure 10: Wind velocity computed on two-dimensional planes from AL-LES downstream of the wind turbine for input to the PE model.

Figures 10 and 11 depict more closely the wind velocity and overall relative SPL on the 2D planes, respectively, downstream from the wind turbine without plotting the entire terrain topography. The actuator lines and source locations are shown in the figures as well. Similarly, Figures 12 and 13 depict more closely the wind velocity and overall relative SPL on the 2D planes, respectively, diagonally at a 50 degree angle away from the wind turbine without plotting the entire terrain topography. The actuator lines and source locations are shown in the figures as well.

Only a single time step at time step = 70, i.e., 136 seconds in real time, is depicted in Figures 10, 11, 12 and 13. Note that the flow fields on the 2D planes are outputted every 100 time steps in the flow solver to reduce the data output size, therefore time step = 70 is actually the 7000 time step in the flow solver where approximately 0.02 seconds is used for each step. The figures can be generated for any time step within the 2-minute real-time simulation period, i.e., anywhere between time step = 1 and 70. For example, see Figures 14 and 15. From comparing Figure 11 with Figure 13, increased overall relative SPL values observed in Figure 11 are due to the presence of the wind turbine wake, showing constructive and destructive interference of ground reflected and direct waves. Such observations are not seen in Figure 13.

4. Conclusions

This paper showed numerical noise propagation calculations of a single wind turbine in complex terrain near a town in Central Denmark. The calculations were performed using high-fidelity tools: large-eddy simulation for the flow and the parabolic equation for the noise propagation. The purpose of the work is to estimate the noise level at increasing distances from a single wind turbine and investigate the effects of complex terrain and the wind turbine wake on noise propagation, which have not been discussed in great detail in the current article. Results indicate

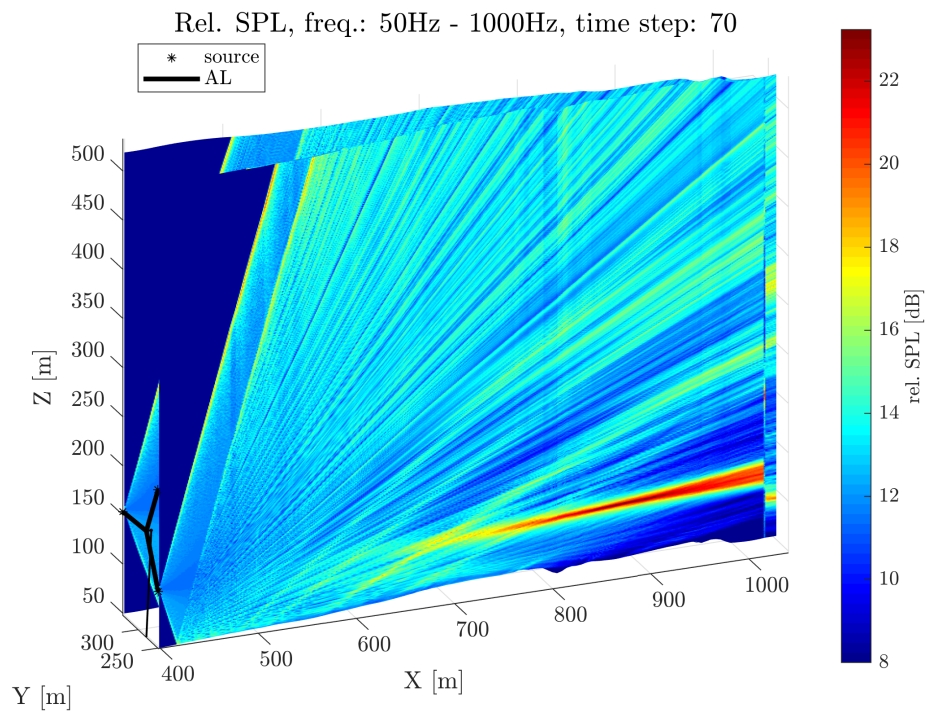


Figure 11: Overall relative sound pressure level (rel. SPL) computed from the PE model downstream of the wind turbine.

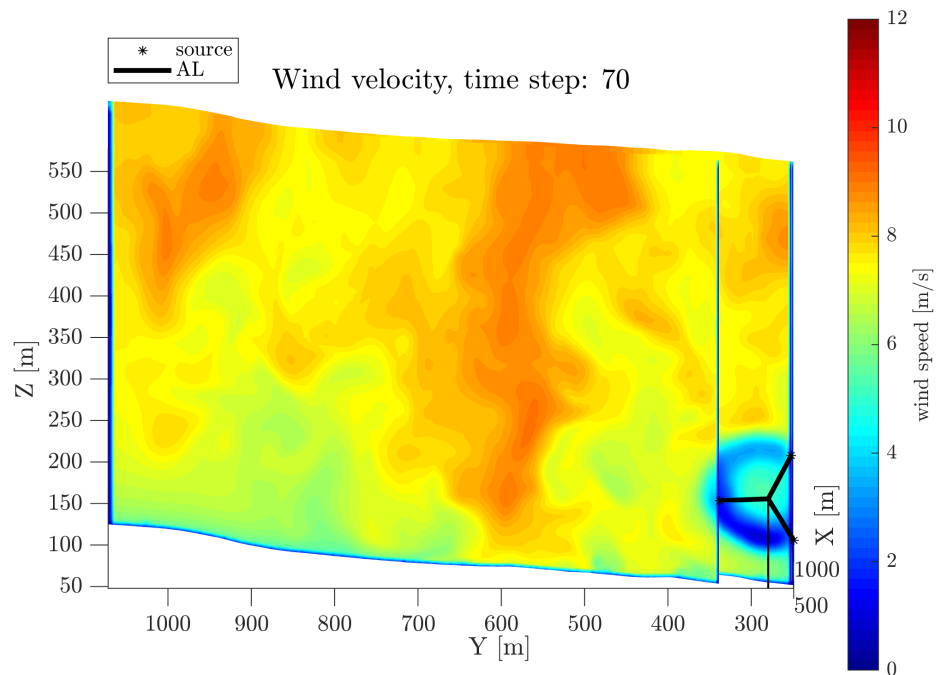


Figure 12: Wind velocity computed on two-dimensional planes from AL-LES diagonally from the wind turbine for input to the PE model.

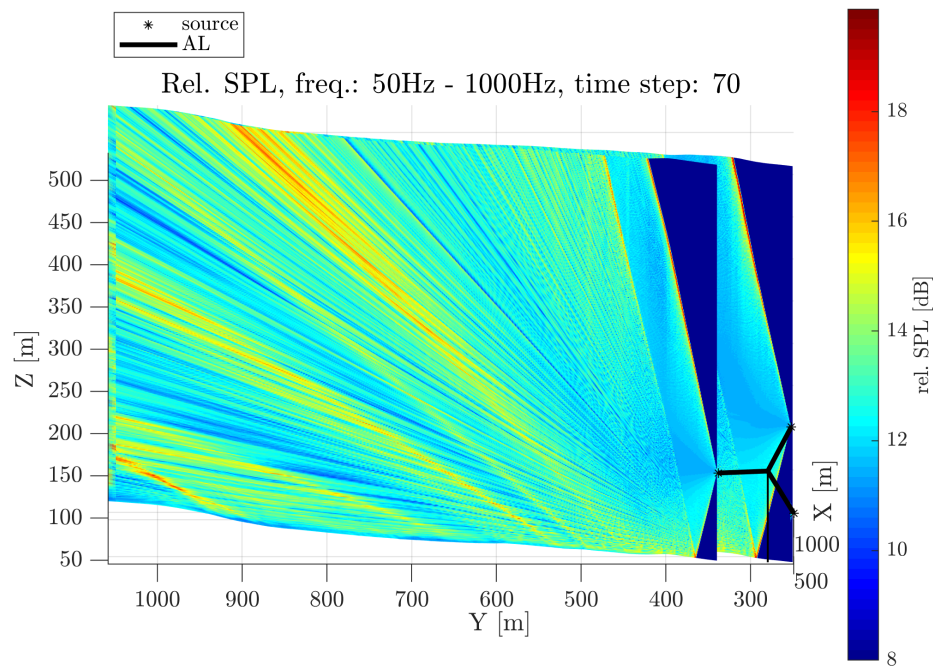


Figure 13: Overall relative sound pressure level (rel. SPL) computed from the PE model diagonally from the wind turbine.

that high-fidelity numerical noise propagation predictions of wind turbines in complex terrain can be done by using computational fluid dynamics and the Technical University of Denmark's noise propagation tool. Soon, comparisons with acoustic measurements and further developments in modeling the wind turbine noise source and propagation will be carried out.

Acknowledgments

Contains data from Styrelsen for dataforsyning og effektivisering (<https://kortforsyningen.dk>): DHM-2007/Terræn (1,6 m grid) retrieved May 15, 2019. Computations were performed on Jess, the high performance computing cluster at Risø Campus, Technical University of Denmark.

Nomenclature

α	atmospheric absorption coefficient
ΔL	relative sound pressure level
ΔL_{sum}	overall relative sound pressure level
δx	spatial resolution for horizontal direction on 2D-plane
δy	spatial resolution for vertical direction on 2D-plane
λ	wavelength of the solving frequency
c	speed of sound
c_{eff}	effective speed of sound
f	frequency
L_p	sound pressure level
L_W	sound power level
N	number of frequencies used
R	rotor radius
r	radial distance from the source

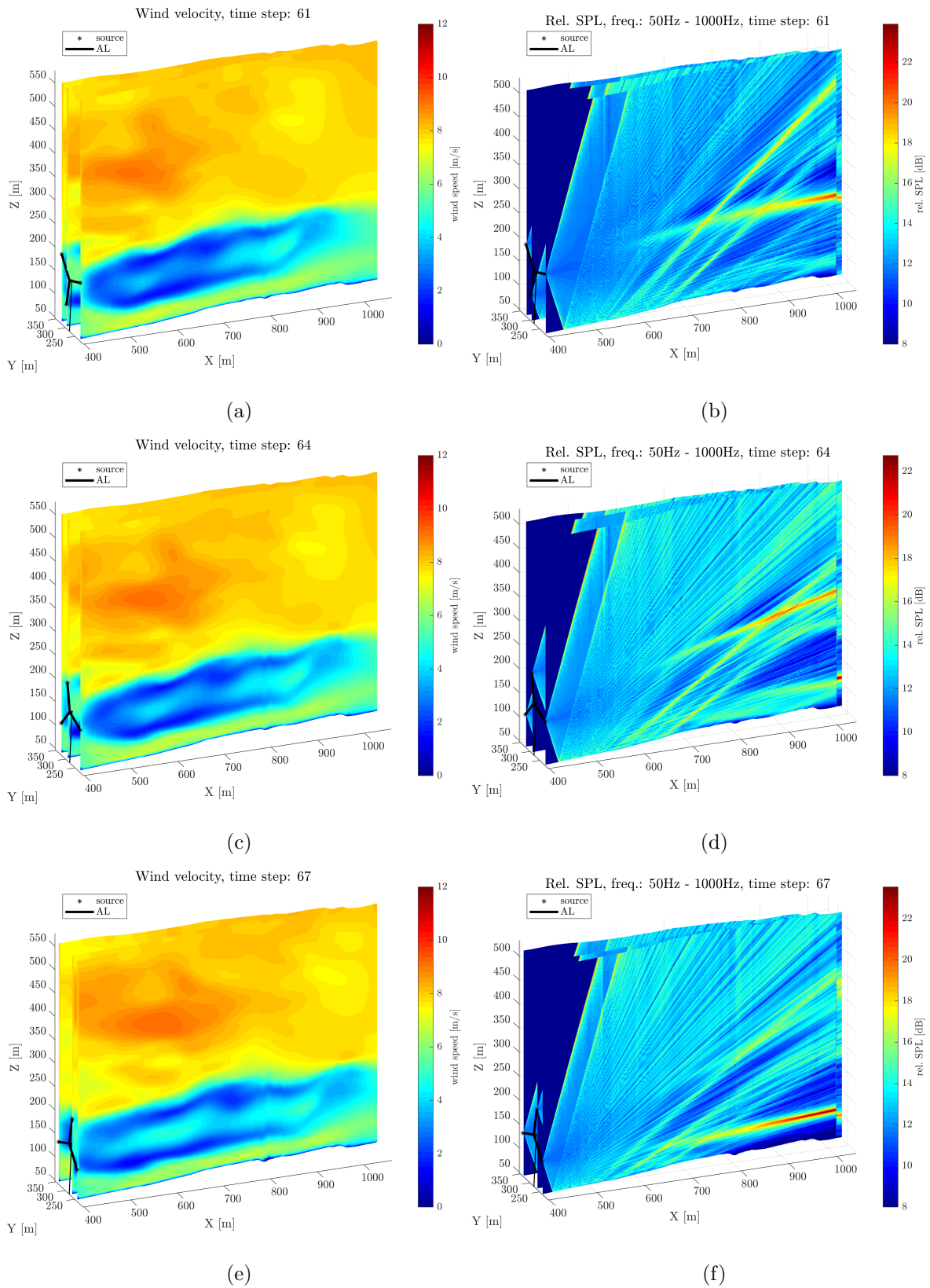


Figure 14: Wind velocity computed on two-dimensional planes from AL-LES downstream of the wind turbine for time steps (a) 61, (c) 64, and (e) 67. Similarly, overall relative sound pressure level (rel. SPL) computed from the PE model for time steps (b) 61, (d) 64, and (f) 67.

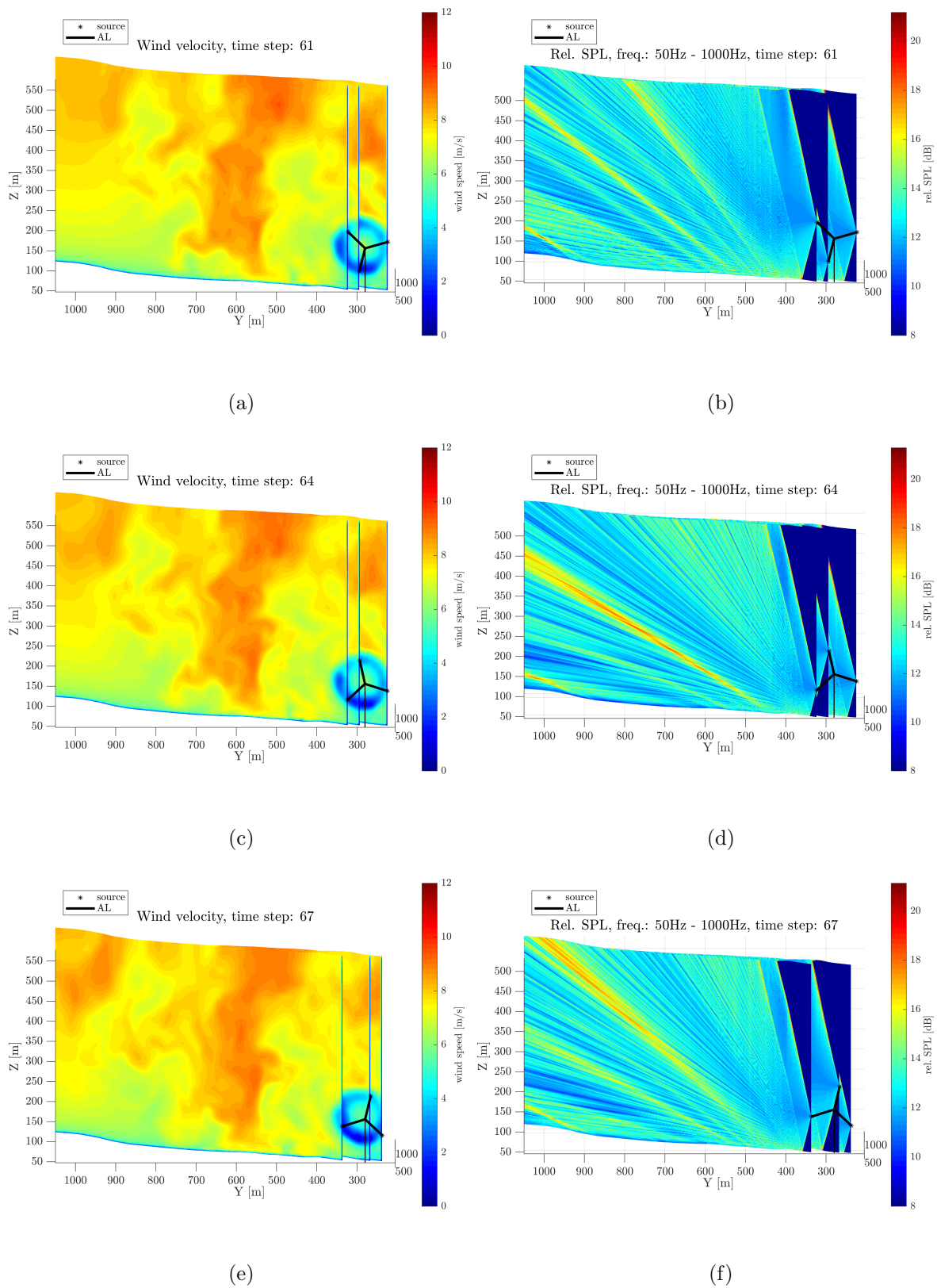


Figure 15: Wind velocity computed on two-dimensional planes from AL-LES diagonally from the wind turbine for time steps (a) 61, (c) 64, and (e) 67. Similarly, overall relative sound pressure level (rel. SPL) computed from the PE model for time steps (b) 61, (d) 64, and (f) 67.

v_x	wind velocity component along direction between source and receiver
X, Y, Z	location in a 3D Cartesian coordinate system
2D	two-dimensional
3D	three-dimensional
AL	actuator line
CFD	computational fluid dynamics
DHM	Danmarks Højdemodel
DTU	Technical University of Denmark
LES	Large-Eddy Simulation
MPI	Message Passing Interface
NREL	National Renewable Energy Laboratory
PE	parabolic equation
RANS	Reynolds-Averaged Navier Stokes
rel.	relative
RPM	revolutions per minute
SPL	sound pressure level
w	normalized streamwise windspeed
WindSTAR-Pro	Wind turbine Simulation Tool for AeRodynamic noise Propagation

References

- [1] Oerlemans S, Sijtsma P and López B M 2007 *Journal of Sound and Vibration* **299** 869 – 883 ISSN 0022-460X URL <http://www.sciencedirect.com/science/article/pii/S0022460X06006316>
- [2] Pedersen E and Kerstin P W 2004 *The Journal of the Acoustical Society of America* **116** 3460–3470 (Preprint <https://doi.org/10.1121/1.1815091>) URL <https://doi.org/10.1121/1.1815091>
- [3] Persson Wayne K and Öhrström E 2002 *Journal of Sound and Vibration* **250** 65 – 73 ISSN 0022-460X URL <http://www.sciencedirect.com/science/article/pii/S0022460X01939057>
- [4] The Danish Ministry of the Environment 2011 Statutory order no. 1284 on noise from wind turbines
- [5] Zhu W J, Cao J, Barlas E, Shen W Z, Zhang L, Sun Z, Yang H and Xu H 2018 *Journal of Physics: Conference Series* **1037** 022002 URL <https://doi.org/10.1088%2F1742-6596%2F1037%2F2%2F022002>
- [6] Shen W Z, Zhu W J, Barlas E and Li Y 2019 *Renewable Energy* **143** 1812 – 1825 ISSN 0960-1481 URL <http://www.sciencedirect.com/science/article/pii/S0960148119308134>
- [7] Cao J, Zhu W, Wu X, Wang T and Xu H 2018 *Energies* **12** ISSN 1996-1073 URL <https://www.mdpi.com/1996-1073/12/1/18>
- [8] Heimann D, Englberger A and Schady A 2018 *Wind Energy* **21** 650–662 (Preprint <https://onlinelibrary.wiley.com/doi/pdf/10.1002/we.2185>) URL <https://onlinelibrary.wiley.com/doi/abs/10.1002/we.2185>
- [9] Heimann D and Englberger A 2018 *Applied Acoustics* **141** 393 – 402 ISSN 0003-682X URL <http://www.sciencedirect.com/science/article/pii/S0003682X18300707>
- [10] Sessarego M, Shen W and Barlas E 2019 *Proceedings of the 8th International Conference on Wind Turbine Noise (INCE/Europe)* URL https://orbit.dtu.dk/files/184733701/SessionD_Propagation2.pdf
- [11] Brooks T, Pope D and Marcolini M 1989 *Airfoil Self-noise and Prediction* NASA reference publication 1218 (National Aeronautics and Space Administration, Office of Management, Scientific and Technical Information Division) URL <https://ntrs.nasa.gov/archive/nasa/casi.ntrs.nasa.gov/19890016302.pdf>
- [12] Styrelsen for Dataforsyning og Effektivisering 2019 DHM-2007/Terræn (1,6 m grid) URL <https://kortforsyningen.dk/>
- [13] Sørensen N N 1994 *General purpose flow solver applied to flow over hills* Ph.D. thesis Technical University of Denmark
- [14] Michelsen J A 1992 Basis3D - a platform for development of multiblock PDE solvers. Tech. rep. Technical University of Denmark
- [15] Sørensen J N and Shen W Z 2002 *Journal of Fluids Engineering* **124** 393–399 ISSN 0098-2202 URL <http://dx.doi.org/10.1115/1.1471361>
- [16] Sørensen J N, Mikkelsen R F, Henningson D S, Ivanell S, Sarmast S and Andersen S J 2015 *Philosophical transactions. Series A, Mathematical, physical, and engineering sciences* **373** 20140071 ISSN 1471-2962 URL <http://www.ncbi.nlm.nih.gov/pmc/articles/PMC4290405/>

- [17] Øye S 1996 *Proceedings of 28th IEA Meeting of Experts Concerning State of the Art of Aeroelastic Codes for Wind Turbine Calculations* (Lyngby: International Energy Agency) pp 71–76
- [18] Jonkman J, Butterfield S, Musial W and Scott G 2009 Definition of a 5-MW reference wind turbine for offshore system development Tech. rep.
- [19] Sessarego M, Shen W Z, Van der Laan M P, Hansen K S and Zhu W J 2018 *Applied Sciences* **8** ISSN 2076-3417 URL <http://www.mdpi.com/2076-3417/8/5/788>
- [20] Hansen M O L 2008 *Aerodynamics of wind turbines* 2nd ed (London: Earthscan)
- [21] Mann J 1994 *Journal of Fluid Mechanics* **273** 141–168 ISSN 1469-7645
- [22] Mann J 1998 *Probabilistic Engineering Mechanics* **13** 269 – 282 ISSN 0266-8920 URL <http://www.sciencedirect.com/science/article/pii/S0266892097000362>
- [23] Brooks T F, Pope D S and Marcolini M A 1989 *NASA Reference publication 1218*
- [24] Bérengier M C, Gauvreau B, Blanc-Benon P and Juvé D 2003 *Acta Acustica united with Acustica* **89** 980–991 ISSN 1610-1928 URL <https://www.ingentaconnect.com/content/dav/aaua/2003/00000089/00000006/art00009>
- [25] West M, Gilbert K and Sack R 1992 *Applied Acoustics* **37** 31 – 49 ISSN 0003-682X URL <http://www.sciencedirect.com/science/article/pii/0003682X9290009H>
- [26] Ostashev V E and Wilson D K 2015 *Acoustics in Moving Inhomogeneous Media* 2nd Edition (CRC Press)
- [27] Cheng R, Morris P J and Brentner K S 2009 *The Journal of the Acoustical Society of America* **126** 1700–1710 (*Preprint* <https://asa.scitation.org/doi/pdf/10.1121/1.3203934>) URL <https://asa.scitation.org/doi/abs/10.1121/1.3203934>
- [28] Barlas E 2017 *Development of an advanced noise propagation model for noise optimization in wind farm* Ph.D. thesis Technical University of Denmark
- [29] Barlas E, Zhu W J, Shen W Z, Kelly M and Andersen S J 2017 *Applied Acoustics* **122** 51 – 61 ISSN 0003-682X URL <http://www.sciencedirect.com/science/article/pii/S0003682X1730172X>
- [30] Barlas E, Zhu W, Shen W, Dag K and Moriarty P 2017 *Acoustical Society of America. Journal* **142** ISSN 0001-4966
- [31] Barlas E, Wu K L, Zhu W J, Porté-Agel F and Shen W Z 2018 *Renewable Energy* **126** 791 – 800 ISSN 0960-1481 URL <http://www.sciencedirect.com/science/article/pii/S0960148118304038>
- [32] Zhu W J, Shen W Z, Barlas E, Bertagnolio F and Sørensen J N 2018 *Renewable and Sustainable Energy Reviews* **88** 133 – 150 ISSN 1364-0321 URL <http://www.sciencedirect.com/science/article/pii/S1364032118300558>
- [33] Attenborough K 1985 *Journal of Sound and Vibration* **99** 521 – 544 ISSN 0022-460X URL <http://www.sciencedirect.com/science/article/pii/0022460X85905383>